ALJEST

CO₂ sorption over B-ZSM-5 templated by a new organic template: Kinetic study

B. Bensafi [1,*], N. Chouat [1], M. Lafjah [1], F. Djafri [1]

[1] Laboratoire de chimie des matériaux, Département de Chimie, Université d'Oran 1 Ahmed Ben Bella, El M'naouer BP: 1524, Oran, Algérie.

* Corresponding author: bensafibb@hotmail.com; Tel: +213 782 185 160.

ARTICLE INFO

ABSTRACT/RESUME

Abstract: ZSM-5 zeolite has a great importance in hazardous substances adsorption and catalytic process. In this study, a borosilicate ZSM-5 zeolite was carried out using N,N-dimethylaniline as a novel structure-directing agent. The synthetized material was characterized by X-ray diffraction, thermal analysis (TG/dTG), N_2 physical adsorption, and Fourier transform infrared spectroscopy. CO_2 adsorption at different temperatures was evaluated by a volumetric method, and both Langmuir and Freundlich adsorption models were applied. According to the experimental results, B-ZSM-5 zeolite has a favorable adsorption behavior at low temperatures. Different kinetic models were used to describe the adsorption of CO_2 over B-ZSM-5. A good agreement with experimental data was found for pseudo-n order.

I. Introduction

Zeolites are crystalline microporous aluminosilicates based on an infinitely extending three-dimensional, four connected framework of AlO_4 and SiO_4 tetrahedral linked each other by sharing an oxygen atom. Each SiO_4 tetrahedron in the framework bears a neutral charge, and each AlO_4 tetrahedron in the framework bears a net negative charge that is balanced by an extra-framework cation, which is usually an alkali or alkaline earth metal [1]. Zeolites are classified according to the number of opening pore, 8 MR (Member of Rings) as small-pore, 10 MR as medium-pore, 12 MR as large-pore, and extra-large pore more than 12 MR systems [2]. Their applications (ion exchange, adsorption, shape selectivity or catalytic activity) are essentially determined by their structures [3], and their aluminum content in the framework [4]. Zeolites include the natural types like chabazite (CHA), erionite (ERI) and clinoptilolite (HEU), and the synthetic types like A (LTA), X and Y (FAU), and ZSM-5 (MFI) [5].

As one of the most important zeolites is ZSM-5 (Zeolite Socony Mobil with sequence number five) from structural type MFI. Its framework structure has bi-directional intersecting channels, one is straight and parallel to [010] direction with 5.1 x 5.7 Å and the other is sinusoidal in [100] direction with 5.4 x 5.6 Å, with an opening of 10-membered ring [6]. It is widely used in adsorption [6] and especially in catalytic process such as alkylation, aromatization, dehydration, and cracking [7-10]. Borosilicate ZSM-5 (B-ZSM-5) zeolites are a class of high silica MFI type where aluminum atoms are substituted by boron atoms. This kind of synthesis was the first conducted by Taramasso *et al.* [11]. Since the physic-chemical properties behavior B-zeolite is different from Al-zeolite, it is expected that substitution of aluminum by boron would modify the acidic properties of zeolites [12].

It is well known that the template plays significant role in the synthesis of zeolites. The template can act as a structure directing agent, space filling and charge compensating species that is required for the successful synthesis of these materials [13,14]. The structure and the size of the organic compound have a significant influence on the obtained materials [15]. The ZSM-5 can be synthesized using different templates such as tetra-alkyl ammonium ions, amines and alcohols [16].

On the other hand, N,N-dimethylaniline is a tertiary amine of aniline derivatives. It is consisted of dimethylamino group attached to a phenyl group. N,N-dimethylaniline and their derivatives are used as a reagent for methyl furfural, as a solvent for manufacturing of vanillin michlers ketones [17], and may be used also as ligands in organometallic chemistry such as 4-formyl-N,N-dimethylaniline [18]. It can be obtained from in-situ hydrogenation of nitrobenzene with hydrogen generated from methanol over Raney-Ni catalyst followed by alkylation. Recently, NNDMA is mostly produced from a two-step process involving the reduction of nitroarenes into anilines and the subsequent alkylation [19]. N,N-dimethylaniline presents very interesting physical properties such a diameter of 0.622 Å and a volume of 76.7 Å^3 [20], that is why it has been chosen as a voluminous molecule to obtain a zeolite with remarkable opening pores and high surface area.

Recently, great attention has been given to adsorption and separation of CO_2. Carbon dioxide is the main greenhouse gas, which causes severe global warming. Its concentration in atmosphere is continuously increasing every year, and therefore is required to remove from Natural and Flue gases for environmental and energy perception. Capture of CO_2 by adsorption has emerged as a potential technology due to low energy requirement and easy application [21]. Industrially, the most used adsorbents are metal–organic frameworks, activated carbons, silica and alumina. In the last recent years, zeolites have been found suitable materials for this polluting gas elimination. Their structure, high surface area and physic-chemical properties such as hydrothermal and mechanical resistant make of them good adsorbents. Therefore, enormous efforts have been made by Scientifics to improve zeolites capture of CO_2 such as the work made by Frantz *et al.* [6], ZSM-5 have been prepared with high sodium content to improve adsorptive properties. Chang Hun Lee *et al.* [22] tested the effect of pore structure on the CO_2 adsorption capacity using three types of organic templates.

In our knowledge, the N,N-dimethylaniline is one of the amines which have not been used as structure-directing agent in MFI structure synthesis. This study presents the first utilization of N,N-dimethylaniline as organic template in synthesis of borosilicate ZSM-5 zeolite and its application for CO_2 capture. In the literature, the Al-ZSM-5 zeolite has been proposed as potential candidate for CO_2 adsorption process [23] due to its high adsorption capacity and facile regeneration. Here, we report the first work that carry out the utilization of the B-ZSM-5 in carbon dioxide adsorption.

II. Experimental Protocole

II.1. Materials

The reagents used were: N,N-dimethylaniline (Sigma-aldrich, 99%) as organic template, porous silica gel powder (Fluka) as silicium source, sodium hydroxide pellets (Sigma-aldrich, 99.998%) as alkaline cation, boric acid (99.999%, Sigma-aldrich) as boron source, and demineralized water purified using Water Purification System Milli-Q (MERCK).

II.2. Characterization

The pH value of the homogenous hydrogel was measured by inoLab pH 730 (WTW). The crystalline structure was determined by X-ray diffraction (Bruker AXS D8 ADVANCE diffractmeter with a CuKα radiation source). Thermal analysis (TG/dTA) experiments were carried out by a TA Micrometrics 2050 TGA apparatus. The porosity occupied by the organic template was released by a calciner (Nabertherm). Textural properties of the material were measured by nitrogen physisorption (Micromeritics ASAP 2020). The FTIR spectra were taken in KBr pellets using Alpha-Bruker FTIR spectrophotometer.

II.3. B-ZSM-5 synthesis

The hydrogel mixture was prepared by the following manner:

3 g of silica gel powder mixed with 0.8 g of sodium hydroxide solution, then 1.815 g N,N-dimethylaniline was added drop wise under stirring in a known volume of demineralized water. One hour later, 1.2 g of boric acid was added to the first mixture. This new mixture was stirred for 24h in room temperature till formation of homogenous hydrogel. After stirring, pH value was taken (pH = 11.68) and the hydrogel was allowed to aging. One hour later, the homogeneous mixture was transferred to a Teflon lined autoclave with a volume full capacity of 50 ml and carried out in crystallization temperature of 423 K under autogenous pressure, for 6 days. After crystallization had been completed the autoclave was rapidly cooled and the recovered white solid was washed with deionized water, filtered off, and then dried at 373 K overnight. The dried zeolite sample was calcined for 6 h under atmospheric air at 773 K to eliminate the organic compound.

II.4. CO_2 adsorption

The carbon dioxide adsorption performance of the B-ZSM-5 sample was evaluated in the pressure range of 5 to 730 mmHg and different temperatures of 273 K, 288 K, and 298 K using CO_2 gas with high purity (99.999 %). The adsorption measurement was carried out on Micromeritics ASAP 2020 apparatus. After each measurement, the adsorbed CO_2 molecules were desorbed by degassing gradually at 623 K for 4 hours to reach a vacuum. In order to investigate the adsorption behavior of the B-ZSM-5 zeolite, two isotherm models were proposed,

Langmuir (Equation (1)) and Freundlich (Equation (2)) [24]:

$$q_e = \frac{q_m K_A P}{(1 + K_A P)} \qquad (1)$$

$$q_e = K_F P^{\frac{1}{n_F}} \qquad (2)$$

Where P: pressure of the gas [mmHg]; q_e: solid phase adsorption quantity of carbon dioxide on zeolite at equilibrium [cm^3 STP/g]; K_A: Langmuir isotherm constant [1/ mm Hg]; K_F: Freundlich isotherm constant; q_m: single layer CO_2 adsorption capacity [cm^3/g]; n_F: factor of heterogeneity.

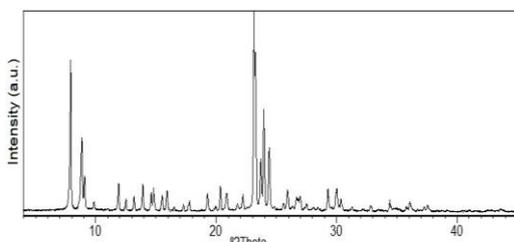## III. Results and discussion

III.1. XRD

Figure 1. *XRD pattern of synthesized B-ZSM-5 zeolite.*

X-ray diffraction (XRD) pattern of the synthesized B-ZSM-5 is illustrated on Figure 1. The reflection peaks are represented between the angles $2\theta = 3°$ and $45°$. According to the results, the main peaks are $2\theta = 7.9, 8.8, 8.9, 23.2, 23.3,$ and $24°$. Comparing to the collection of simulated XRD MFI-type zeolite [25], our synthesized B-ZSM-5 have the same peaks with high pure crystallinity and without any impurities.
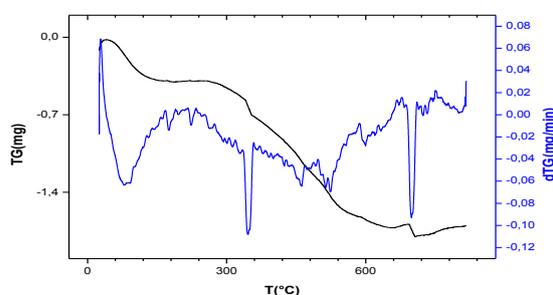
III.2. Thermal analysis

Figure 2. *TG/dTG curves of synthesized B-ZSM-5 zeolite.*

The thermogravimetric analysis (TG/dTG) curves of the prepared zeolite are shown in Figure 2.

The zeolite was heated from room temperature to 830 °C, at 10 °C/min, with 100 ml/min under air. The total mass lost was 1.8 mg. It represents both water and organic template losses. The first stage of weight loss was identified between 40 °C and 150 °C, that it is related to desorption of water molecules. In the first step, weakly bound water molecules are lost, while some stronger ones are lost gradually. After this stage we see stable level until the temperature of 280 °C. In this range there was any loss. The second stage was observed between 280 °C and 640 °C and it is related to mass loss caused by the thermodegradation of the organic template. At temperatures above 640 °C, weight loss is associated with to thermofusion process of the zeolite.

III.3. BET

Figure 3 shows N_2 adsorption-desorption isotherm of the sample B-ZSM-5. This isotherm provides valuable information on the textural properties of B-ZSM-5. For many microporous materials, in particular zeolites, the utilization of nitrogen at liquid temperature (77 K) is recommended. The specific surface area (S_{BET}) was evaluated by BET method using adsorption data in the range of a relative pressure from $p/p^0 = 0.05$ to $p/p^0 = 0.29$. The t-plot method was applied to determine the volume of micropores (V_{mic}). The adsorbed amount at relative pressure $p/p^0 = 0.98$ reflects the total adsorption capacity (V_{tot}). The void volume (V_{int}) account for the volume of interstices among zeolite particles. The values of determined textural properties are summarized in Table 1.
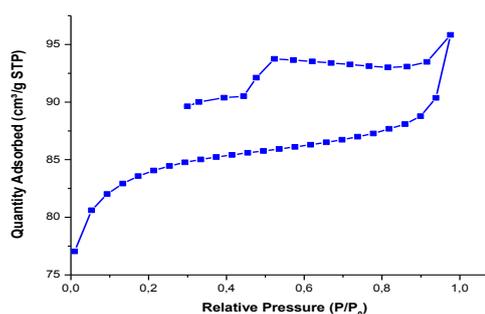

Figure 3. *Nitrogen adsorption-desorption isotherm at 77 K of B-ZSM-5.*

Table 1. *Textural properties of the zeolite B-ZSM-5.*

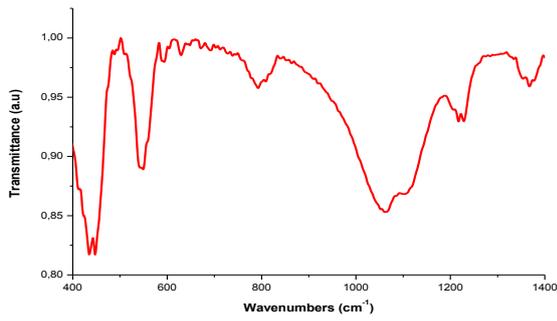| S_{BET} (m²/g)	S_{ext} (m²/g)	S_{mic} (m²/g)	V_{mic} (cm³/g)	V_{voi} (cm³/g)	V_{tot} (cm³/g)
255.6	11.02	244.58	0.13	93.61	93.74

III.4. FTIR spectrum

Figure 4. FTIR spectrum of synthesized B-ZSM-5 zeolite.

FTIR spectrum of the synthesized sample is illustrated on Figure 4. Characteristics bands of ZSM-5 are shown in the spectrum. The bands at the regions of 1225 cm^{-1} and 1085 cm^{-1}, are respectively for external and internal asymmetrical stretching. For the external symmetrical stretching, characteristic band is around of 792 cm^{-1}. The five-member ring of pentasil structure of ZSM-5 zeolite is confirmed by the vibrational band at 549 cm^{-1} [26]. Absorption bands at 1367 cm^{-1} and 629 cm^{-1} are attributed to stretching vibrations of the tetra-coordinated framework boron, and Si-O-B symmetric bending [27], respectively. Finally, the band near to 450 cm^{-1} is attributed to the T-O bending vibration internal tetrahedral units of the SiO$_4$ [28].

III.5. CO$_2$ adsorption

As mentioned on Figure 5, the CO$_2$ adsorption over B-ZSM-5 zeolite at different temperatures 273 K, 288 K, and 298 K shows a regular variation of adsorbed amounts until upper pressure limit (730 mmHg) with an optimal adsorption capacity of 2.05 mmol/g. From curves, it is shown that adsorption is an inverse function of temperature, since; adsorption is reducing with increasing of temperature. It is important to mention that similar behavior of reduction in the adsorption of CO$_2$ at higher temperature has been observed in literature although with porous adsorbents materials and zeolites [29,30].

It is expected that borosilicate ZSM-5 zeolite has higher affinity with CO$_2$ molecules; it is due to the substitution of aluminum atoms by boron atoms into the ZSM-5 framework. It develops a low acidity in the zeolite lattice which can helps it in adsorption of CO$_2$ as acid gas. Interactions among the pores and the surface of B-ZSM-5 zeolite and the large quadruple moment of CO$_2$ have been pointing out as the factor which is responsible for the good uptake capacity found in this material.
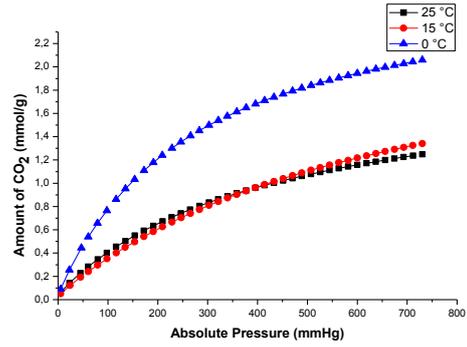

Figure 5. Carbon dioxide adsorption at different temperatures.

III.6. Langmuir and Freundlich models

The study of equilibrium is indispensable throughout all adsorption process. The experimental determination and modeling adsorption capacities of an adsorbent constitute the initial step to any adsorption process sizing. For this, two different isotherms models were tested, Langmuir and Freundlich.

The Langmuir model is based on simple assumptions (absence of interactions between adsorbed molecules, sites are energetically equivalent, and contain just one molecule adsorbed). Linearization of Langmuir equation (Equation (1)) is written as follows:

$$\frac{1}{q} = \frac{1}{q_m K_A} x \frac{1}{P} + \frac{1}{q_m} \qquad (3)$$

Freundlich model considers that there are different types of energy of different adsorption sites. The linearization of its equation (Equation (2)) is written as follows:

$$ln\, q = ln(K_F) + \frac{1}{n_F} ln(P) \qquad (4)$$

The Langmuir and Freundlich isotherm models fitting parameters, for the three different temperatures analyzed in this study and calculated respectively by Equation (3) and Equation (4), are summarized in Table 2. According to the results shown in the Table 2, Freundlich model is more suitable than Langmuir for the two temperatures 288 K and 298 K. This is justified by the values of the regression coefficients which are high ($R^2 = 0.9969$, 0.9937 for Freundlich model, and $R^2 = 0.9529$, 0.9477 for Langmuir model at both temperatures 288 K and 298 K, respectively). However, at 273 K, the Langmuir model ($R^2 = 0.9860$) is more favorable than Freundlich model ($R^2 = 0.9773$), this is justified by their regression coefficients. So we can conclude at temperatures 288 K and 298 K adsorptions takes place on various kinds of sites with different energies, while the adsorption at 273 K is carried out on the same sites energy and each site can sets a single molecule of CO2.

Table 2. Langmuir and Freundlich constants at different temperatures.

Temperature [K]	Langmuir			Freundlich		
	q_m [mmol/g]	K_A (10^{-4}) [1/mmHg]	R^2	K_F (10^{-4})	n_F	R^2
273	1.9193	89.66	0.9860	437.87	1.6526	0.9773
288	0.9567	100.24	0.9529	150.76	1.4492	0.9969
298	0.9327	136.66	0.9477	237.35	1.6289	0.9937

III.7. Selection of the kinetic model

According to the literature, a large number of kinetic models [31] have been proposed to describe the adsorption process of different adsorbents. In this work, to choose a suitable kinetic model, variable models have been tested, such pseudo-first order (Equations (5)), pseudo-second order (Equations (6)), and pseudo-n order (Equations (7)) [32,33,24].

- Pseudo-first order

$$\frac{dq_t}{dt} = k_f (q_e - q_t) \qquad (5)$$

After integration for limit conditions $q_t = 0$ at $t = 0$ and $q_t = q_e$ at $t = t$, Equation (5) can be written as follows (Equation (5')):

$$ln(q_e - q_t) = -k_f\, t + ln\, q_e \qquad (5')$$

- Pseudo-second order

$$\frac{dq_t}{dt} = k_s (q_e - q_t)^2 \qquad (6)$$

After integration for limit conditions, Equation (6) can be written as follows (Equation (6')):

$$\frac{t}{q_t} = \frac{1}{k_s \cdot q_e^2} + \frac{t}{q_e} \qquad (6')$$

- Pseudo-n order

$$\frac{dq_t}{(q_e - q_t)^n} = k_n\, dt \qquad (7)$$

After integration for limit conditions, Equation (7) can be written as follows (Equation (7')):

$$(q_e - q_t)^{1-n} = q_e^{1-n} + k_n (n-1)t \qquad (7')$$

Where q_e [mmol] and q_t [mmol] are respectively adsorption capacities at equilibrium and at time t [min], k_f pseudo-first order kinetic constant [min^{-1}], k_s pseudo-second order kinetic constant [min^{-1}], and k_n pseudo-n order kinetic constant [min^{-1}].

The kinetic model parameters for the CO_2 adsorption at 273 K which was consistent with the fitting results shown on Figure 6 are summarized in the Table 3. It can be observed that pseudo-n order had better results than other models. The utilization of the theoretical equation based on Avrami's model [34] leads to a value of n equal to 0.551 with minimal value of $(q_{e(exp)} - q_{e(theo)})$ and regression coefficient (R^2) superior to 0.99, thus attributed a good correlation between the theoretical model and experimental data. From these results, it can be concluated that the reaction is complexe or multi pathway and the pseudo-n order model is the best for determining adsorption rate.

Table 3. Kinetic model parameters for CO_2 adsorption on B-ZSM-5 zeolite at 273 K.

Pseudo order	Kinetic order	K	$q_{e(exp)}$	$q_{e(theo)}$	R^2
pseudo-first order	1	0.0666	2.0582	245.11	0.9133
pseudo-second order	2	0.0261	2.0582	0.3038	0.2702
pseudo-n order	0.551	0.0425	2.0582	1.5308	0.9975

Pseudo-first order   y = - 0.0666 x + 5.5017
R² = 0.9133

Pseudo-second order   y = - 3.2914 x + 414.24
R² = 0.2702

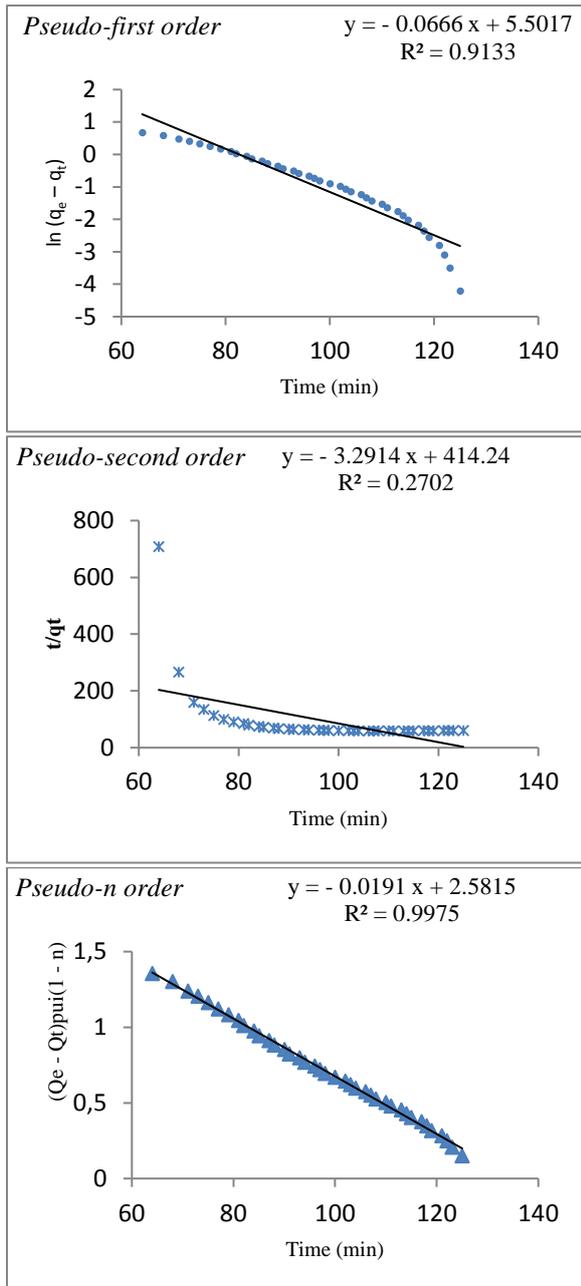**Pseudo-n order**   y = - 0.0191 x + 2.5815
R² = 0.9975

Figure 6. Pseudo-first second and n order kinetic models for CO_2 adsorption at 273 K.

IV. Conclusion

B-ZSM-5 was successfully synthesized using N,N-dimethylaniline as novel organic template. The synthetized sample has a high specific surface area which makes of it a good adsorbent. The zeolite had favorable behavior during CO_2 adsorption especially at 273 K. This behavior was related to condensation of CO_2 in pores and external surface of the adsorbent. It has been found that Langmuir adsorption model is best than Freundlich adsorption model at 273 K to have the highest regression coefficient value, which explains that the adsorption has been done on the same sites energy and each site can sets a single molecule of CO_2. The kinetic models have been applied to confirm the experimental results of CO_2 adsorption on B-ZSM-5. The pseudo-n order model (n = 0.551) validated all experimental results as its R^2 value is near of 1.

V. References

1. Deepak, F.L.; Mayoral, A.; Arenal, R. Advanced Transmission Electron Microscopy: Applications to Nanomaterials, Springer International Publishing, Switzerland, 2015, pp. 94.

2. Busca, G.; Heterogeneous Catalytic Materials: Solid State Chemistry, 1st Edition, Surface Chemistry and Catalytic Behaviour, Elsevier B.V., 2014, pp. 199.

3. Xie, D.; McCusker, L.B.; Baerlocher, C. Structure of the Borosilicate Zeolite Catalyst SSZ-82 Solved Using 2D-XPD Charge Flipping. Journal of the American Chemical Society 133 (2011) 20604–20610.

4. Van Bekkum, H.; Flanigen, E.M.; Jansen, J.C. Introduction to zeolite science and practice, Studies in Surface Science and Catalysis, Elsevier Science Publishers B.V., 58, 1991, pp. 298.

5. Kulprathipanja, S. Zeolites in Industrial Separation and Catalysis, WILEY-VCH Verlag GmbH & Co KGaA, Weinheim, 2010, pp. 35.

6. Frantz, T.S.; Ruiz, W.A.; da Rosa, C.A.; Mortola, V.B. Synthesis of ZSM-5 with high sodium content for CO2 adsorption. Microporous and Mesoporous Materials 222 (2016) 209–217.

7. Hu, H.; Zhang, Q.; Cen, J.; Li, X. High suppression of the formation of ethylbenzene in benzene alkylation with methanol over ZSM-5 catalyst modified by platinum. Catalysis Communications 57 (2014) 129–133.

8. Zhang, X.; Lin, L.; Zhang, T.; Liu, H. Catalytic dehydration of lactic acid to acrylic acid over modified ZSM-5 catalysts. Chemical Engineering Journal 284 (2016) 934–941.

9. Tshabalala, T.E.; Scurrell, M.S. Aromatization of n-hexane over Ga, Mo and Zn modified H-ZSM-5 zeolite catalysts. Catalysis Communications 72 (2015) 49–52.

10. Zhao, X.; Wei, L.; Cheng, S.; Huang, Y.; Yu, Y.; Julson, J. Catalytic cracking of camelina oil for hydrocarbon biofuel over ZSM-5-Zn catalyst. Fuel Processing Technology 139 (2015) 117–126.

11. Abrishamkar, M.; Azizi, S.N.; Kazemian, H. Synthesis of borosilicate MFI type zeolite using different aging techniques. Chemistry of Metals and Alloys 3 (2010) 12–17.

12. Bandyopadhyay, R.; Kubota, Y.; Sugimoto, N.; Fukushima, Y.; Sugi, Y. Synthesis of borosilicate zeolites by the dry gel conversion method and their characterization. Microporous and Mesoporous Materials 32 (1999) 81–91.

13. Álvaro-Muñoz, T.; Márquez-Álvarez, C.; Sastre, E. Use of different templates on SAPO-34 synthesis: Effect on the acidity and catalytic activity in the MTO reaction. Catalysis Today 179 (2012) 27–34.

14. Yin, C.; Wei, Y.; Wang, F.; Chen, Y. Introduction of mesopority in zeolite ZSM-5 using resin as templates. Materials Letters 98 (2013) 194–196.

15. Sang, S.; Chang, F.; Liu, Z.; He, C.; He, Y.; Xu, L. Difference of ZSM-5 zeolites synthesized with various templates. Catalysis Today 93-95 (2004) 729–734.

ALJEST

16. Thubsuang, U.; Ishida, H.; Wongkasemjit, S.; Chaisuwan, T. Novel template confinement derived from polybenzoxazine-based carbon xerogels for synthesis of ZSM-5 nanoparticles via microwave irradiation. Microporous and Mesoporous Materials 156 (2012) 7–15.

17. Gowrisankar, M.; Venkateswarlu, P.; Kumar, K.S.; Sivarambabu, S. Volumetric, speed of sound data and viscosity at (303.15 and 308.15) K for the binary mixtures of N,N-dimethylaniline + aliphatic ketones (C3–C5), +4-methyl-2-pentanone, +acetophenone, +cyclicketones. Journal of Industrial and Engineering Chemistry 20 (2014) 405–418.

18. Packianathan, S.; Raman, N. Stimulated DNA binding by metalloinsertors having the 4-formyl-N,N-dimethylaniline Schiff base: Synthesis and characterization. Inorganic Chemistry Communications 45 (2014) 55–60.

19. Shimizu, K.; Shimura, K.; Nishimura, M.; Satsuma, A. Direct Synthesis of N-Substituted Anilines from Nitroaromatics and Alcohols under H2 by Alumina-Supported Silver Cluster Catalysts. ChemCatChem 3 (2011) 1755–1758.

20. Marcus, Y.; The Properties of Solvents, Wiley Series in Solution Chemistry, volume 4, John Wiley & Sons Ltd, 1998, pp. 92.

21. Sengupta, S.; Amte, V.; Dongara, R.; Das, A.K.; Bhunia, H.; Bajpai, P.K. Effects of the Adsorbent Preparation Method for CO2 Capture from Flue Gas Using K2CO3/Al2O3 Adsorbents. Energy Fuels 29 (2015) 287–297.

22. Lee, C.H.; Hyeon, D.H.; Jung, H.; Chung, W.; Jo, D.H.; Shin, D.K.; Kim, S.H. Effects of pore structure and PEI impregnation on carbon dioxide adsorption by ZSM-5 zeolites. Journal of Industrial and Engineering Chemistry 23 (2015) 251–256.

23. Wirawan, S.K.; Creaser, D. CO2 Adsorption on Silicalite-1 and Cation Exchanged ZSM-5 Zeolites using a Step Change Response Method. Microporous and Mesoporous Materials 91 (2006) 196–205.

24. Chalal, N.; Bouhali, H.; Hamaizi, H.; Lebeau, B.; Bengueddach, A. CO2 sorption onto silica mesoporous materials made from nonionic surfactants.

25. Treacy, M.M.J.; Higgins, J.B. Collection of Simulated XRD Powder Patterns for Zeolites, Fifth Revised Edition, Elsevier B.V., 2007, pp. 276.

26. Li, C.; Wu, Z. handbook of zeolite science and technology, Microporous Materials Characterized by Vibrational Spectroscopies, chapter 11, 2003.

27. Thibault-Starzyk, F.; LES MATÉRIAUX MICRO ET MÉSOPOREUX: Caractérisation, Groupe français des zéolithes, EDP Sciences, 2004, pp. 61.

28. Jiang, J.; Duanmu, C.; Yang, Y.; Gu, X.; Chen, J. Synthesis and characterization of high siliceous ZSM-5 zeolite from acid-treated palygorskite. Powder Technology 251 (2014) 9–14.

29. Sheikh, M.A.; Hassan, M.M.; Loughlin, K.F. Adsorption equilibria and rate parameters for nitrogen and methane on Maxsorb activated carbon. Gas Separation and Purification 10 (1996) 161–168.

30. Cavenati, S.; Grande, C.A.; Rodrigues, A.E. Adsorption Equilibrium of Methane, Carbon Dioxide, and Nitrogen on Zeolite 13X at High Pressures. Journal of Chemical and Engineering Data 49 (2004) 1095–1101.

31. Song, G.; Zhu, X.; Chen, R.; Liao, Q.; Ding, Y.D.; Chen, L. An investigation of CO2 adsorption kinetics on porous magnesium oxide. Chemical Engineering Journal 283 (2016) 175–183.

32. Lagergren, S.; Svenska, B.K.; Handl, V. Removal of Arsenite and Arsenate Ions from Aqueous Solution by Basic Yttrium Carbonate. Water Research 30 (1996) 1143–1148.

33. Ho, Y.S.; McKay, G. Sorption of dyes and copper ions onto biosorbents. Process Biochemistry 38 (2003) 1047–1061.

34. Lopes, E.C.N.; dos Anjos, F.S.C.; Vieira, E.F.S.; Cestari, A.R. An alternative Avrami equation to evaluate kinetic parameters of the interaction of Hg (II) with thin chitosan membranes. Colloid Interface Science 263 (2003) 542–547.

Please cite this Article as:
Bensafi B., Chouat N., Lafjah M., Djafri F., *CO2 sorption over B-ZSM-5 templated by a new organic template: Kinetic study, Algerian J. Env. Sc. Technology, 3*:3 (2017) 67-73